

Article

# Influence of the Aspect Ratio of Sodium Iron Titanate Whiskers on the Mechanical and Tribological Performances of Fluorocarbon Composite Coatings

Jiazhi Zhang <sup>1</sup>, Chang Li <sup>1</sup> , Kelan Yan <sup>1</sup>, Liming Shen <sup>1,\*</sup> and Ningzhong Bao <sup>1,2,\*</sup>

<sup>1</sup> State Key Laboratory of Material-Oriented Chemical Engineering, College of Chemical Engineering, Nanjing Tech University, Nanjing 210009, China; 1084070459@njtech.edu.cn (J.Z.); changli@njtech.edu.cn (C.L.); liyan@njtech.edu.cn (K.Y.)

<sup>2</sup> Institute of Graphene, Jiangsu Industrial Technology Research Institute, Nanjing 210009, China

\* Correspondence: lshen@njtech.edu.cn (L.S.); nzhbao@njtech.edu.cn (N.B.); Tel./Fax: +86-25-8317-2244 (N.B.)

Received: 10 September 2019; Accepted: 17 October 2019; Published: 20 October 2019



**Abstract:** Inorganic–organic composite coatings with fluoroethylene vinyl ether (FEVE) resin as polymer matrix and sodium iron titanate (NFTO) whiskers with different aspect ratios as reinforcement filler are prepared by the liquid-phase blending method. The influence of aspect ratio and content of NFTO whiskers on the morphology, and the mechanical and tribological performances, of NFTO-reinforced FEVE composite coatings are investigated. The addition of NFTO whiskers can obviously enhance the mechanical and wear resistance performances of the composite coatings and reduce the friction coefficient. The worn surface and wear debris of the composite coatings are studied with scanning electron microscopy (SEM) to reveal the friction-reducing and wear resistance mechanisms. The composite coating filled with ~10 wt.% NFTO whiskers has the best wear resistance performance, since the monodispersed hard whisker can carry the load applied on the sliding surface and reduce the adhesive wear of the polymer matrix. Among the three types of NFTO whiskers, the whiskers with a medium aspect ratio show the best reinforcement effect since they provide the optimum mechanical support to the polymer matrix and cannot be pulled out from the matrix easily.

**Keywords:** fluorocarbon coating; sodium iron titanate whisker; surface modification; mechanical performances; tribological behaviors

## 1. Introduction

Polymeric coatings have been widely applied in various industrial fields, such as marine equipment, construction, automobiles, etc., to improve the surface performance of products [1,2]. The solvent soluble fluorine-olefin/vinyl ether copolymer (FEVE) coating, as a main branch of advantaged fluorocarbon polymers, has a variety of outstanding characteristics, including chemical resistance, weather resistance, and ambient temperature curability [3–5]. Nevertheless, similar to other polymeric coatings, FEVE coating is susceptible to erosion and abrasive wear, resulting in the appearance of plastic deformation and crack initiation, and thus impairs the protection and barrier performance of the coating [6,7]. Accordingly, improving the mechanical strength and wear resistance performance of FEVE coating is of great practical significance.

Inorganic–organic composites have attracted significant attention by introducing hard reinforcement fillers or friction-reducing fillers to improve the hardness, stiffness, compressive strength, and wear resistance performance of matrix [8,9]. The commonly used inorganic fillers or micro/nano particles include carbon nanotubes, glass fibers, MoS<sub>2</sub>, and ceramics [10,11]. Additionally, their chemical composition, sizes, shapes, and filling content can be tuned to meet the requirement of

different application fields. Among numerous inorganic fillers, titanium-based whiskers have attracted significant attention owing to their excellent mechanical strength, wear resistance, and chemical and thermal stability [12,13]. Xie et al. [8] investigated the enhanced tribological performance of potassium titanate whisker (PTW) incorporated polyetheretherketone (PEEK) / polytetrafluoroethylene (PTFE) composites. Zhuang et al. [14] prepared PTW/PEEK composites and demonstrated that PTW has a significant reinforcement effect on the mechanical performance of polymer matrix. Liu et al. [15] chose nanoscale PTW (AX-301) with a large aspect ratio as the functional filler to prepare composites with excellent thermal reflectivity and insulation performance. Feng et al. [16] chose PTW as fillers to improve the crystallization and tribological performance of PTFE. Nevertheless, the influence of the aspect ratio of titanium-based fillers on the tribological and mechanical performances of polymeric composites remains relatively unexplored [17–19].

In the present work, sodium iron titanate (NFTO)/FEVE composite coatings are prepared by the method of liquid-phase blending, with various contents and aspect ratios of modified NFTO whiskers as the hard reinforcement filler. The main objective of this work is to compare the mechanical and tribological performances of fluorocarbon composite coatings reinforced by whisker shaped titanium-based fillers with different aspect ratios. The wear resistance mechanism regarding different contents and aspect ratios of whiskers are discussed and revealed. The present results can provide some practical guidance for developing polymeric protective coatings with excellent wear resistance performance which is suitable for different application environments.

## 2. Materials and Methods

### 2.1. Reagents and Materials

FEVE resins (JF-2X) were purchased from Changshu 3F Fluorochemical Industry Co. Ltd. (Changshu, China). Polyisocyanate curing agent (N3390) was purchased from Bayer (Bayer, Germany). Butyl acetate was purchased from Sinopharm Chemical Reagent Co. Ltd. (Shanghai, China). Propylene glycol monomethyl ether acetate (99.0%) was obtained from Aladdin Chemical Reagents Company (Shanghai, China). Absolute ethanol (>99.7%) was purchased from Wuxi Yasheng Chemical Co. Ltd. (Wuxi, China). Vinyl tris( $\beta$ -methoxyethoxy) silane (A172, >98%) was purchased from Shanghai Yuanye Biotechnology Co. Ltd. (Shanghai, China). Glacial acetic acid ( $\geq$ AR) was provided by Shanghai Lingfeng Chemical Reagent Co. Ltd. (Shanghai, China). Carbon steel sheets (150 mm  $\times$  70 mm  $\times$  1 mm) were purchased from Kunshan Xinheng Precision Mold Hardware Co. Ltd. (Kunshan, China).

Three types of NFTO whiskers with different aspect ratios were prepared with the molten salt method in the laboratory. To prepare the Whisker L (NFTO whiskers with a large aspect ratio),  $\text{FeTiO}_3$  was used as the iron source. The raw materials with the molar ratio of  $\text{FeTiO}_3/\text{TiO}_2/\text{Na}_2\text{CO}_3 = 1.3:2:1$ , and the molten salt NaCl with the molar mass 4 times of the raw materials were mixed and then sintered at 900 °C for 4 h. Once finished sintering, the product was cooled to room temperature, washed with water, and dried at a temperature of 60 °C for 24 h to obtain the Whisker L sample. The Whisker M (NFTO whiskers with a medium aspect ratio) was prepared with the same procedure, but the iron source was replaced by  $\text{Fe}_2\text{O}_3$ . To prepare the Whisker S (NFTO whiskers with a small aspect ratio),  $\text{FeTiO}_3$  was still the iron source, but KCl-NaCl (1:1) was used, and the sintering temperature was increased to 1000 °C. Other preparation conditions, such as the molar ratio of raw materials and the sintering duration, were consistent with the preparation procedure of Whisker L and Whisker M. The standard X-ray diffraction (XRD) characteristic pattern of NFTO whiskers ( $\text{NaFeTiO}_4$ ) is PDF#33-1255 [20].

### 2.2. Surface Modification of Three Types of NFTO Whiskers

Ten grams of NFTO whiskers were first added into a 50 mL mixture of ethanol and water (the volume ratio of ethanol/water = 9:1) and the pH value of the solution was adjusted to 4 using glacial acetic acid. Then, a certain amount of silane coupling agent A172 (0.05, 0.1, 0.2, 0.3, 0.5, or 0.8 g) was added into the mixture, followed by 30 min of ultrasonic agitation. After forming a uniform

suspension, the sample was moved into an oil bath and kept at 100 °C with mechanical agitation till the solvent of suspension was completely evaporated. The A172 modified NFTO whiskers were obtained after sieving the dried sample.

### 2.3. Preparation of NFTO/FEVE Composite Coatings via the Liquid-Phase Blending Method

NFTO/FEVE composite coatings were prepared via the liquid-phase blending method. First, FEVE resin, butyl acetate, and propylene glycol monomethyl ether acetate were mixed in a 250 mL beaker and the mixture was agitated at 2500 rpm for 30 min to become a homogeneous solution. Then, a certain content of NFTO whiskers (0, 2.5, 5.0, 7.5, 10.0, 12.5, or 15.0 wt.%) and polyisocyanate curing agent (the mass ratio of curing agent/FEVE resin = 1:5) were added into the solution. After being stirred for another 30 min at 2500 rpm, the mixed solution was finally evacuated to remove air bubbles, forming coating paint.

In a typical procedure of preparing a coating, a certain amount of the coating paint was dropped on the surface of a freshly polished steel substrate. The brush of a wire bar coater (ZBQ 100/200/300/400, Pusheng Testing Instrument Co. Ltd. (Shanghai, China)) uniformly spread the paint over the substrate at a constant sliding speed (~150 mm/s) to make a uniform coating [21,22]. The wet film thickness of the coating was 400 µm. The isocyanate groups in the polyisocyanate curing agent could cross-link with the hydroxyl groups in the FEVE resin, resulting in the curing of the coating, as shown in Figure S1. After being cured for 72 h at room temperature, an NFTO/FEVE composite coating with a uniform thickness of 40 ± 5 µm was obtained.

### 2.4. Mechanical Performance Tests

The adhesion performance of the as-prepared NFTO/FEVE composite coatings was tested according to the GB/T 9286-1998 [23] grid test method. A multi-blade cutter (QHF002, Pusheng Testing Instrument Co. Ltd., Shanghai, China) was used to cut uniform meshes on the coating at a uniform speed. Then, a piece of scotch tape was stuck on to cover the coating and then quickly peeled off. The adhesion performance of the coating was determined by the peeling degree of the coating from its steel substrate. Grade 0 represents the best adhesion performance, when no coating peeled off the steel substrate at all; and Grade 5 represents the worst adhesion result with more than 65% of the area of the coating partially or completely peeled off.

The hardness of the as-prepared composite coatings was tested according to the GB/T 6739-2006 [24] pencil method (QHQ-A-750, Flora Automatic Technology Co. Ltd. (Tianjin, China)). A pencil with the lowest hardness (9B) was fixed in the test instrument to keep the bottom of the instrument parallel to the coating surface, which was placed on a horizontal table. The pencil tip slightly touched the surface of the coating and left traces on it when the test instrument was driven through the coating surface at a speed of 0.5–1 mm/s. If there was no indentation left on the coating surface after erasing the pencil mark, then the test was repeated with a pencil of higher hardness. The hardness of the coating was defined according to the hardest pencil the coating could stand without leaving an indentation longer than 3 mm on the surface of the coating.

The impact resistance performance of the as-prepared composite coatings was determined using the GB/T 1732-1993 [25] impact test method (QCJ-50, Shanghai Meiyu Instrument Equipment Co. Ltd., Shanghai, China). The coating was placed face up or face down on the sample holder to undergo a positive or negative impact generated by a hammer falling from a certain height. The impact resistance of the coating was defined by the most powerful force that did not cause cracks on the coating surface.

### 2.5. Tribological Property Tests

The friction and wear behaviors of the NFTO/FEVE composite coatings were tested on a multifunctional material surface performance tester (CFT-I, Lanzhou Zhongke Kaihua Technology Development Co. Ltd., Lanzhou, China)). All the tests were conducted under the dry sliding friction condition at room temperature. A steel ball (4 mm in diameter, under 3 N load) moved in a linear

reciprocating fashion on the coating surface at a fixed speed of 500 r/min and a reciprocating amplitude of 5 mm for 15 min. For comparison, the same tests were also carried out on FEVE coatings.

### 2.6. Other Characterizations

The microstructures of the cross-section, worn surface, and wear debris of coatings were studied with scanning electron microscopy (Nova Nano SEM 450, FEI, Hillsboro, OR, USA). X-ray diffraction (XRD, D8-Advance, Bruker, Germany), operating at 40 kV and 40 mA with the scan range of  $5^{\circ}$ – $70^{\circ}$  ( $2\theta$ ) and scanning rate of  $10^{\circ}/\text{min}$ , was used to characterize the crystalline phase and structure of NFTO whiskers. Fourier transform infrared (FT-IR) spectra were collected using a RQUINOX55 spectrometer (Nicolet IS10, Beijing, China) to study the functional groups on the surface of modified NFTO whiskers. The contact angle measuring instrument (SDC-350, SINDIN, Guangdong, China) was used to evaluate the wettability on the surface of the NFTO whiskers. To measure the contact angle of the unmodified and modified NFTO whiskers, samples were flatly filled up in a fixed Teflon ring. After 6  $\mu\text{L}$  of distilled water was dropped on the sample surface, a photo was immediately taken for measurement.

## 3. Results and Discussion

### 3.1. Morphology and Aspect Ratio Distribution of NFTO Whiskers

Three types of NFTO whiskers were used as the reinforcement fillers to prepare FEVE composite coatings. Figure 1 shows the SEM images of as-prepared whiskers with a slender needle-shape morphology. Whisker L has an average length of  $\sim 12 \mu\text{m}$ , and the corresponding diameter is  $\sim 0.5 \mu\text{m}$ , as shown in Figure 1a. Whisker M has a relatively short and thick morphology, with a length varying from 8 to 9  $\mu\text{m}$  and the diameter is about 0.8–0.9  $\mu\text{m}$ , as shown in Figure 1b. Whisker S has the shortest length in the three types of NFTO whiskers, with an average length of  $\sim 2 \mu\text{m}$ , and the corresponding diameter is 0.3–0.4  $\mu\text{m}$ , as shown in Figure 1c.

The aspect ratios of the three types of NFTO whiskers, calculated based on the statistic results, are shown in Figure 1d. In order to get an accurate statistical result, about five SEM images (200–300 whisker specimens) were used for each type of NFTO whiskers. The aspect ratio of the majority of Whisker L falls in the range of 22 to 26, and the corresponding fraction in this range is about 70%. The aspect ratio of most of Whisker M falls in the range of 7 to 14, and the corresponding fraction in this range is about 60%. The aspect ratio of the majority of Whisker S falls in the range of 3 to 7, and the corresponding fraction in this range is about 80%.

The phase composition and purity of the three types of NFTO whiskers were identified by XRD patterns. As shown in Figure 1e, the diffraction patterns of the three NFTO whiskers are consistent with the standard pattern of  $\text{NaFeTiO}_4$  (PDF#33-1255), indicating the excellent phase purity of prepared samples. The relative strong peak intensities of NFTO whiskers also implies the good crystallinity of prepared whiskers. It is noteworthy that the (112) crystal face of the three samples is slightly different in peak intensity from that in the standard pattern, which can be attributed to the preferential growth of NFTO whiskers. In addition, the characteristic signals of unreacted reactants ( $\text{Na}_2\text{CO}_3$ ) or intermediate phase ( $\text{Fe}_2\text{O}_3$ ) have not appeared, indicating the complete conversion of raw materials [20].

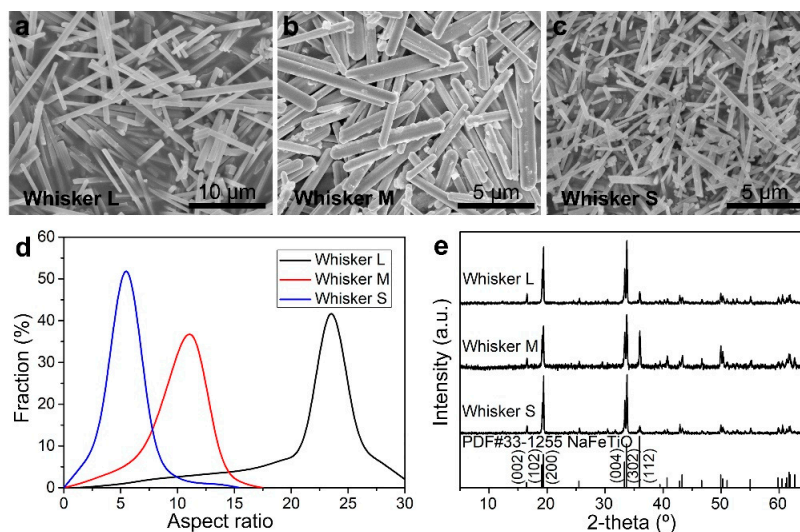


**Figure 1.** (a–c) SEM images, (d) aspect ratio distribution, and (e) XRD patterns of three types of sodium iron titanate (NFTO) whiskers.

### 3.2. Chemical Modification of NFTO Whiskers

In order to obtain hydrophobic NFTO whiskers and improve their dispersity in FEVE resin, the three types of NFTO whiskers were modified by different contents of coupling agent A172. Figure 2 shows the contact angle results of modified and unmodified whiskers. The unmodified NFTO whiskers (0 wt.% of A172) are highly hydrophilic, with a contact angle of  $\sim 30^\circ$ . After being modified with A172, for all three types of NFTO whiskers, the contact angle quickly increases as the content of A172 rises to 1 wt.%, then gradually reaches the maximum value around 3 wt.%, and finally shows a very slight decline with the further addition of A172. When the content of A172 is no more than 3 wt.%, the hydroxyl groups on the whisker surface dehydrate with the silanol groups on A172; thus, the hydrophobicity of whiskers can be improved. An excess content of A172 may cause the polymerization of coupling agent molecules, which can affect the reaction between the A172 and the whisker's surface, resulting in slightly less hydrophobicity and a smaller contact angle. Therefore, 3 wt.% of A172 is the optimum amount for the surface modification of NFTO whiskers, and the contact angles of modified whiskers are  $143.1^\circ$ ,  $139.3^\circ$ , and  $141.6^\circ$ , respectively, for Whisker L, Whisker M, and Whisker S. Figure S2 shows the dispersibility of the three types of NFTO whiskers in butyl acetate, the diluent of FEVE resin, before and after the surface modification with A172. It can be seemed that the modified whiskers can be well dispersed in the solvent.

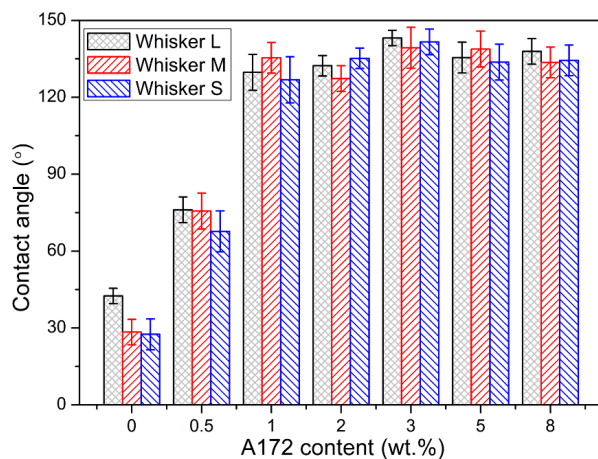


**Figure 2.** The contact angles of three types of NFTO whiskers modified with different contents of coupling agent A172.

The modification mechanism of coupling agent A172 on the surface of NFTO whiskers is shown in Figure 3. The reaction process can be divided into three steps. (i) In the presence of water, the alkoxy groups on A172 are prone to hydrolyze and generate silanols. Since the alkoxy groups can hydrolyze at a high rate, alcohol needs to be added in the reaction mixture to inhibit the hydrolysis rate. (ii) The dehydration condensation of the formed silanols with the large amount of hydroxyl groups on the surface of NFTO whiskers leads to the formation of a Si–O–Ti bond, and thus the coupling agent can be grafted on the whisker's surface. (iii) The vinyl groups at the end of the coupling agent molecular chain combine with the FEVE resins by forming hydrogen bonds. Meanwhile, the silanols on the coupling agent molecules can combine with each other and form a network-like film, covering the surface of the whisker and realizing its surface modification [26]. In the FT-IR spectra of the modified NFTO whiskers, as shown in Figure S3, the peak at  $1323\text{ cm}^{-1}$ , corresponding to the Si–O–Ti bond and the characteristic peak of vinyl  $\text{CH}_2=\text{CH}-\text{R}$  at  $1568\text{ cm}^{-1}$ , are both observed, indicating that the whisker has been successfully modified with A172.

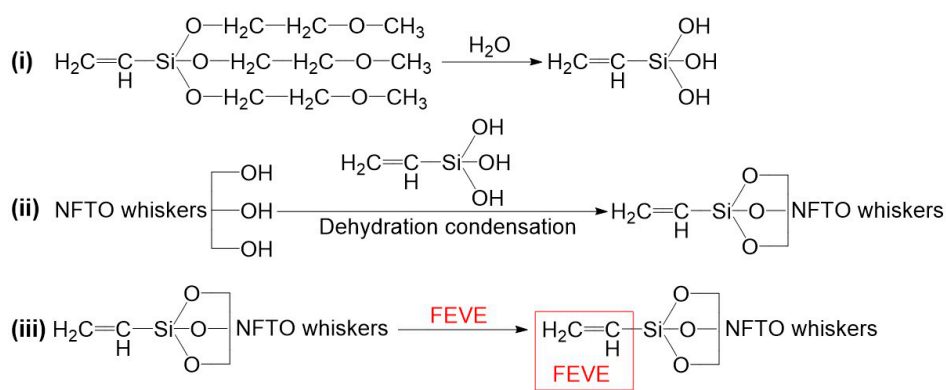


**Figure 3.** Schematic illustration of the modification mechanism of coupling agent A172 on the surface of NFTO whiskers. (i) The hydrolysis of coupling agent A172, (ii) the dehydration condensation of coupling agent with whiskers, and (iii) the combination of coupling agent A172 and fluoroethylene vinyl ether (FEVE) resin.

### 3.3. The Cross-Sectional Morphology of NFTO/FEVE Composite Coatings

The dispersibility of the modified NFTO whiskers in FEVE resins can be evaluated with the cross-sectional morphology of composite coatings. The cross-section of the FEVE coating is very smooth, and almost no wrinkles, holes, or other defects are noticeable, as shown in Figure S4. Figure 4 shows the cross-sectional SEM images of the three types of NFTO/FEVE composite coatings filled with different types of NFTO whiskers. For the NFTO/FEVE composite coatings filled with 5 wt.% whiskers, as shown in Figure 4(a1, b1, c1), the cross-sections of all the three coatings are coarse because of the addition of fillers. The filled whiskers are distributed in matrix without agglomeration or formation of obvious structural defects, indicating that the modified whiskers have an excellent dispersibility in resin matrix due to the surface modification of  $\text{CH}_2$  groups [11]. There are few small holes observed in each SEM image, and they are left behind by the whiskers which were pulled out while the coatings were frozen in nitrogen and broken for SEM samples.

With the increase of the whisker's content to 10 wt.%, as shown in Figure 4(a2, b2, c2), the filled whiskers are still evenly dispersed in matrix, but structural defects have appeared, especially in Whisker S, as shown in Figure 4(c2). For the composite coatings filled with 15 wt.% whiskers, as shown in Figure 4(a3, b3, c3), more structural defects are observed, and some whiskers have stacked together. The severe stacking of filler whiskers at a high filling concentration is also observable in the optical images of their coatings, as shown in Figure S5. The above results indicate that the whisker content has reached a saturated state, and the further increase of the filler concentration may cause an attenuation of the integral properties of composite coatings.

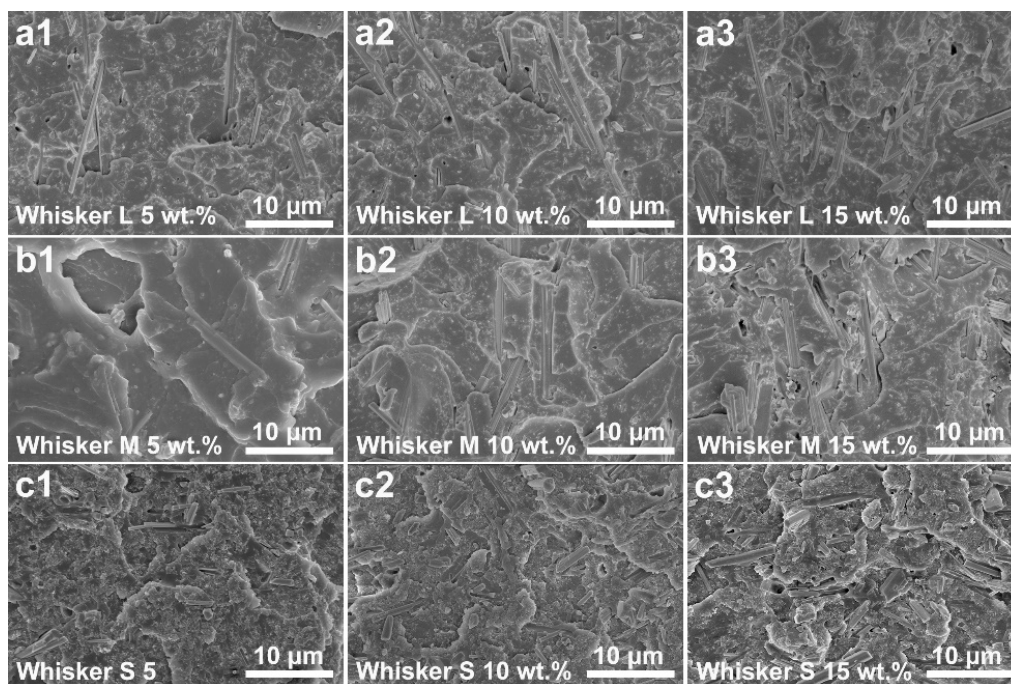


**Figure 4.** Cross-sectional SEM images of NFTO/FEVE composite coatings filled with different contents of (a,a1,a2) Whisker L, (b,b1,b2) Whisker M, and (c,c1,c2) Whisker S. The filled content of NFTO whiskers is (a1,b1,c1) 5 wt.%, (a2,b2,c2) 10 wt.%, and (a3,b3,c3) 15 wt.%.

### 3.4. Mechanical Performances of the NFTO/FEVE Composite Coatings

The filler concentration dependent mechanical performances (adhesion, hardness, and impact resistance) of the three types of NFTO/FEVE composite coatings filled with Whisker L, M, and S, respectively, are shown in Figure 5. Compared with the performance of the FEVE coating, the adhesion, hardness, and positive impact resistance of the NFTO/FEVE composite coatings are significantly increased, from Grade 4 to Grade 2, 1 H to 3 H, and 0.98 to 1.57 N-s, respectively, as shown in Figure 5a–c. It implies that the modified NFTO whiskers have good interface interaction with the matrix, and they indeed reinforce the mechanical strength of the composite coatings. The influence of the whisker content and the aspect ratio on the adhesion, hardness, and positive impact resistance of composite coatings were not found, but the negative impact resistance of composite coatings was greatly improved. The enhancement extent is dependent on the content of whiskers. The addition of a small amount of NFTO whiskers plays a supporting role in the impact process, thus can significantly improve the negative impact resistance of composite coatings. However, the steel substrate is under the direct impact from the hammer and is easier to deform due to its low toughness. The composite coating with a higher filler content of NFTO whiskers has less extensibility and so cracks will form, resulting in an attenuated negative impact resistance.

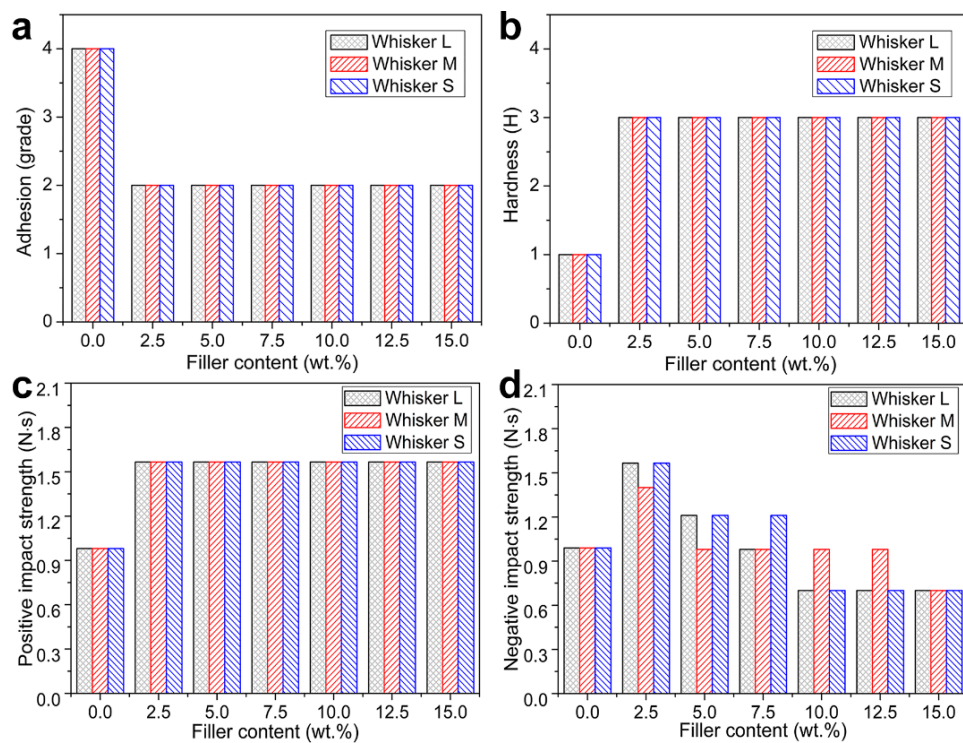


**Figure 5.** Mechanical performances of the pure FEVE coating and three types of NFTO/FEVE composite coatings with different fill contents. (a) Adhesion performance, (b) hardness, (c) positive impact strength, and (d) negative impact strength.

### 3.5. Tribological Behaviors of NFTO/FEVE Composite Coatings

The change of friction coefficient and wear volume loss of the NFTO/FEVE composite coatings filled with different contents and aspect ratios of NFTO whiskers are shown in Figure 6. The average friction coefficient of the pure FEVE coating is 0.934 and it is significantly reduced with the addition of NFTO whiskers, as shown in Figure 6a. The friction component generated by adhesion is equal to the product of the actual contact area between the polymeric matrix and the metal counterpart and the shear stress of soft material [27]. With the addition of NFTO whiskers, the hard reinforcement fillers can carry the load applied on the sliding surface directly and reduce the real contact area of the polymer matrix with the metal counterpart, resulting in a significantly reduced friction coefficient of the NFTO/FEVE composite coatings [28].

For the composite coatings filled with Whisker L, the friction coefficient first decreases with the increase of whisker content till 10 wt.%, with the lowest average friction coefficient of 0.656, and then increases with the filler content, as shown in Figure 6a. The increase of the content of NFTO whiskers causes a larger abrasive force to the metal counterpart, resulting in the increase of the friction coefficient. When the content of Whisker L is 15 wt.%, the average friction coefficient reaches 0.791. The wear volume loss evolution of composite coatings filled with different contents of whiskers also illustrates the reinforcement effect of inorganic whiskers. The wear volume loss of the unfilled FEVE coating is  $0.170 \text{ mm}^3$ , as shown in Figure 6b. For the composite coatings filled with Whisker L, the wear resistance first increases with the content of Whisker L, and then decreases. When the content of Whisker L is 10 wt.%, the composite coating reaches the lowest wear volume loss value ( $0.007 \text{ mm}^3$ ), a 95.9% reduction from the unfilled FEVE coating. The wear resistance performance of NFTO whiskers filled composites is far better than that of other reported coatings filled with titanium-based whiskers [8,16].

The composite coatings filled with Whisker M have a lower friction coefficient, compared with that filled with Whisker L, as shown in Figure 6a. Different from the whiskers with a large aspect ratio, which are easier to be broken under an external force, resulting in a larger abrasive force, Whisker M

has a medium aspect ratio, and therefore can result in a better friction-reducing effect on the composite coatings. The composite coating reaches the smallest friction coefficient value (0.608) when the content of Whisker M is 5.0 wt.%. The wear volume loss of composite coatings filled with Whisker M is very similar to that with Whisker L, as shown in Figure 6b.

Compared with Whisker L and Whisker M filled composite coatings, the composite coatings filled with Whisker S have higher friction coefficients and wear volume losses, as shown in Figure 6a,b, indicating the worst friction-reducing and wear resistance effect. We speculate that the NFTO whiskers with a small aspect ratio have a relatively weak binding force with the polymer matrix, and thus can be separated from the matrix easily. In addition, the load-carrying capability of Whisker S is relatively weak, and so the whiskers can be squeezed out from the matrix and torn apart together with wear debris by the means of adhesive wear [29].

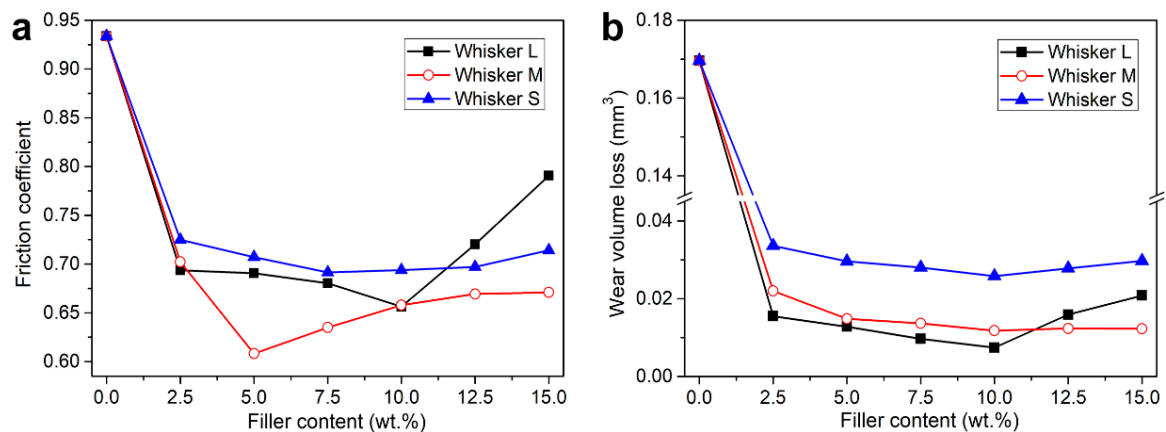


**Figure 6.** (a) Friction coefficient and (b) wear volume loss of the unfilled FEVE coating and NFTO/FEVE composite coatings filled with different contents of Whisker L, Whisker M, and Whisker S.

Figure 7 shows the SEM images of the worn surface and wear debris of the unfilled FEVE coating and NFTO/FEVE composite coatings filled with different contents of Whisker L, Whisker M, and Whisker S. The surface of the unfilled FEVE coating is subjected to adhesive wear, and so the worn surface is rough and has large numbers of cracks, as shown in Figure 7(a1). The high adhesion force between the matrix and steel counterpart results in the high friction coefficient of the unfilled coating. The flake-like debris with a large size can be torn apart from the matrix, as shown in Figure 7(a2), resulting in the severe wear volume loss.

Compared with the unfilled FEVE coating, the worn surface of NFTO/FEVE composite coatings filled with Whisker L turned smoother and no cracks appeared, as shown in Figure 7(b1,7c1, d1). When the contents of Whisker L are 5 wt.% and 10 wt.%, no obvious holes and defects can be observed on the worn surface, indicating that the filled whiskers can carry the applied load effectively and reduce the adhesive wear of matrix. While for the composite coatings filled with 15 wt.% Whisker L, structural defects and holes have appeared, indicating that the whiskers were enriched in the composite coating, which caused adhesive wear on the surface. The wear debris is a product of friction experiments and its morphologies and sizes are closely related to the wear resistance performance of the composite coatings. The wear debris images of NFTO/FEVE composite coatings filled with different contents of Whisker L are shown in Figure 7(b2,7c2,7d2). All the wear debris shows a flake-like morphology with a size smaller than that from the pure FEVE coating, indicating the excellent wear resistance performance of the NFTO/FEVE composite coatings.

Compared with the Whisker L filled composite coatings, the composite coatings filled with Whisker M show a smoother worn surface, and almost no signs of plastic deformation and adhesion can be detected, as shown in Figure 7(e1, f1, g1), indicating that the main wear mechanism is minor abrasion. The worn surface of the composite coating filled with 10 wt.% Whisker M has the smoothest worn surface, as well as the finest debris, indicating the excellent reinforcement effect of the monodispersed

whiskers with a medium aspect ratio. Meanwhile, the wear debris of composite coatings filled with 15 wt.% Whisker M have a larger and more uniform morphology than that with a lower fill content, indicating that the partial stacking of whiskers may cause the severe localized adhesive wear.

The worn surfaces of Whisker S filled composite coatings show the plastic deformation of matrix, indicating that the whiskers with a short length cannot carry the load applied on the sliding surface, as shown in Figure 7(h1, i1, j1). More defects and holes appeared on the worn surface of the composite coating filled with 15 wt.% Whisker S. It seems that the whiskers were enriched in the composite coatings and caused severe adhesive wear on the surface. Meanwhile, the wear debris size of the Whisker S filled composite coatings decreases with the increase of fill content, as shown in Figure 7(h2, i2, j2). At a low fill content, the whiskers with a short length cannot support the matrix effectively and attenuate the adhesive wear of the counterpart on the matrix, and thus, large pieces of wear debris can be torn apart from the polymer matrix. With the increase of the fill content, the extruded short whiskers act as third-body abrasive particles, resulting in the formation of wear debris with fine morphology.

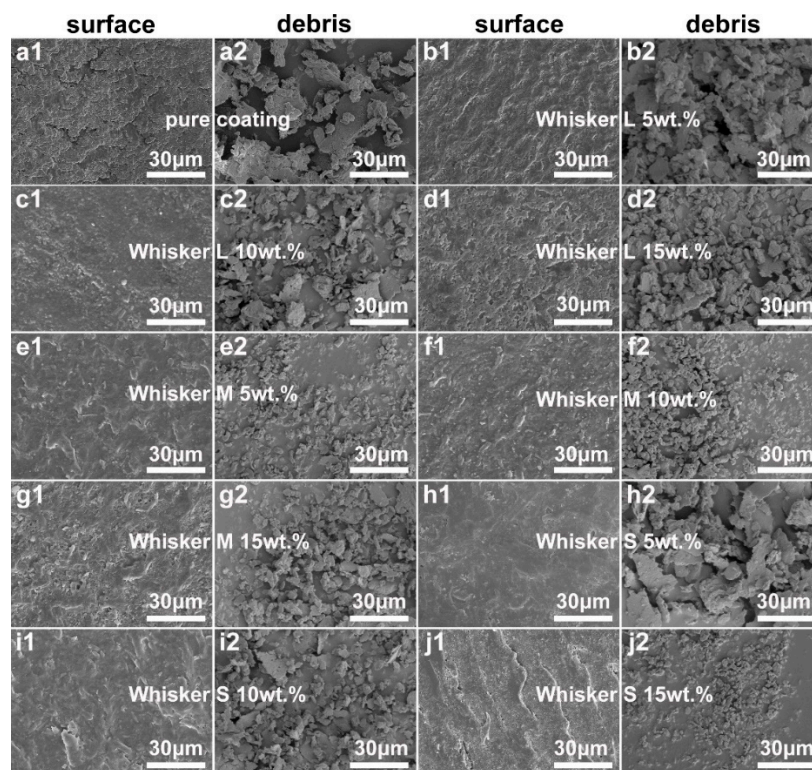


**Figure 7.** SEM images of the worn surface and wear debris of (a1,a2) the pure FEVE coating and (b1–j1,b2–j2) NFTO/FEVE composite coatings. (b1,b2) 5 wt.%, (c1,c2) 10 wt.%, and (d1,d2) 15 wt.% of Whisker L; (e1,e2) 5 wt.%, (f1,f2) 10 wt.%, (g1,g2) 15 w.% of Whisker M; (h1,h2) 5 wt.%, (i1,i2) 10 wt.%, (j1,j2) 15 wt.% of Whisker S.

#### 4. Conclusions

The addition of modified NFTO whiskers can enhance the mechanical and tribological performances of FEVE coatings significantly. With the whisker filling content of ~10 wt.%, the prepared composite coatings exhibited the optimum friction-reducing and wear resistance performances, as the monodispersed hard whiskers can carry the load applied on the sliding surface and reduce the adhesive wear of polymer matrix. The appearance of partially stacked whiskers at a high filler content deteriorates the structural strength of the composite coatings, resulting in a degraded wear resistance performance. Meanwhile, the composite coatings filled with Whisker M have the optimum friction-reducing and wear resistance performance, as Whisker M processes the best mechanical support to the polymer matrix and cannot be pulled out from the matrix easily.

**Supplementary Materials:** The following are available online at <http://www.mdpi.com/2079-6412/9/10/683/s1>, Figure S1: The cross-linking mechanism of the isocyanate groups in the polyisocyanate curing agent with the hydroxyl groups in the FEVE resins, Figure S2: Optical images of the unmodified and modified NFTO whiskers dispersed in butyl acetate. (a, a1) Unmodified and modified Whisker L, (b, b1) unmodified and modified Whisker M, and (c, c1) unmodified and modified Whisker S, Figure S3: FT-IR spectra of the unmodified and modified NFTO whiskers, Figure S4: Cross-sectional SEM image of a pure FEVE coating, Figure S5: Microscope images of NFTO/FEVE composite paints filled with three types NFTO whiskers: (a1–a3) Whisker L, (b1–b3) Whisker M, and (c1–c3) Whisker S. The fill contents of NFTO whiskers are (a1, b1, c1) 5 wt.%, (a2, b2, c2) 10 wt.%, and (a3, b3, c3) 15 wt.%.

**Author Contributions:** Conceptualization, L.S. and N.B.; methodology, J.Z.; software, J.Z.; validation, J.Z. and C.L.; formal analysis, J.Z. and C.L.; investigation, J.Z.; resources, J.Z. and C.L.; data curation, J.Z. and C.L.; writing—original draft preparation, J.Z., C.L., and K.Y.; writing—review and editing, L.S. and N.B.; visualization, L.S. and N.B.; supervision, L.S. and N.B.; project administration, K.Y.; funding acquisition, L.S. and N.B.

**Funding:** This research was supported by the National Natural Science Foundation of China (No. 51425202, No. 51772150), the Natural Science Foundation of Jiangsu Province (BK20160093), and the Project Funded by the Priority Academic Program Development of Jiangsu Higher Education Institutions (PAPD).

**Conflicts of Interest:** The authors declare no conflict of interest.

## References

1. Klaas, N.V.; Marcus, K.; Kellock, C. The tribological behavior of glass filled polytetrafluoroethylene. *Tribol. Int.* **2005**, *38*, 824–833. [[CrossRef](#)]
2. Lin, L.Y.; Kim, D.E. Tribological properties of polymer/silica composite coatings for microsystems applications. *Tribol. Int.* **2011**, *44*, 1926–1931. [[CrossRef](#)]
3. Takayanagi, T.; Yamabe, M. Progress of fluoropolymers on coating applications: Development of mineral spirit soluble polymer and aqueous dispersion. *Prog. Org. Coat.* **2000**, *40*, 185–190. [[CrossRef](#)]
4. Zhou, J.; Tan, Z.; Liu, Z.; Jing, M.; Liu, W.; Fu, W. Preparation of transparent fluorocarbon/TiO<sub>2</sub>-SiO<sub>2</sub> composite coating with improved self-cleaning performance and anti-aging property. *Appl. Surf. Sci.* **2017**, *396*, 161–168. [[CrossRef](#)]
5. Li, Y.; Liu, Y.; Zuo, Y.; Chi, W.; Liu, B.; Shen, Z. Effects of dispersants on dispersion of carbon nanotubes and properties of fluorocarbon resin nanocomposites. *J. Mater. Sci.* **2008**, *43*, 3738–3741. [[CrossRef](#)]
6. Jiang, X.; Wang, J.; Shen, J.; Li, R.; Yang, G.; Huang, H. Improvement of adhesion strength and scratch resistance of fluorocarbon thin films by cryogenic treatment. *Appl. Surf. Sci.* **2014**, *288*, 44–50. [[CrossRef](#)]
7. Wang, Y.; Lim, S. Tribological behavior of nanostructured WC particles/polymer coatings. *Wear* **2007**, *262*, 1097–1101. [[CrossRef](#)]
8. Xie, G.Y.; Zhuang, G.S.; Sui, G.X.; Yang, R. Tribological behavior of PEEK/PTFE composites reinforced with potassium titanate whiskers. *Wear* **2010**, *268*, 424–430. [[CrossRef](#)]
9. Gao, Y.; Picot, O.T.; Bilotti, E.; Peijs, T. Influence of filler size on the properties of poly (lactic acid) (PLA)/graphene nanoplatelet (GNP) nanocomposites. *Eur. Polym. J.* **2017**, *86*, 117–131. [[CrossRef](#)]
10. Yeo, S.M.; Polycarpou, A.A. Tribological performance of PTFE-and PEEK-based coatings under oil-less compressor conditions. *Wear* **2012**, *296*, 638–647. [[CrossRef](#)]
11. Shi, Y.; Feng, X.; Wang, H.; Lu, X. The effect of surface modification on the friction and wear behavior of carbon nanofiber-filled PTFE composites. *Wear* **2008**, *264*, 934–939. [[CrossRef](#)]
12. Kumar, M.; Satapathy, B.K.; Patnaik, A.; Kolluri, D.K.; Tomar, B.S. Hybrid composite friction materials reinforced with combination of potassium titanate whiskers and aramid fibre: Assessment of fade and recovery performance. *Tribol. Int.* **2011**, *44*, 359–367. [[CrossRef](#)]
13. Wang, J.; Shen, L.; Bao, N. Morphology control and characteristic parameter R of molten-salt-synthesized K<sub>2</sub>Ti<sub>6</sub>O<sub>13</sub> whiskers. *J. Mater. Sci.* **2019**, *54*, 10620. [[CrossRef](#)]
14. Zhuang, G.S.; Sui, G.X.; Meng, H.; Sun, Z.S.; Yang, R. Mechanical properties of potassium titanate whiskers reinforced poly (ether ether ketone) composites using different compounding processes. *Compos. Sci. Technol.* **2007**, *67*, 1172–1181. [[CrossRef](#)]
15. Liu, G.; Liu, Y.; Zhao, X. Effects of the potassium titanate functional filler types on the thermal protection performance of heat resistant ablative coated fabrics. *Nano* **2018**, *13*, 1850014. [[CrossRef](#)]
16. Feng, X.; Diao, X.; Shi, Y.; Wang, H.; Sun, S.; Lu, X. A study on the friction and wear behavior of polytetrafluoroethylene filled with potassium titanate whiskers. *Wear* **2006**, *261*, 1208–1212. [[CrossRef](#)]

17. Cho, K.H.; Cho, M.Y.; Kim, S.J.; Jang, H. Tribological properties of potassium titanate in the brake friction material; morphological effects. *Tribol. Lett.* **2008**, *32*, 59–66. [[CrossRef](#)]
18. Shi, Y.J.; Feng, X.; Wang, H.Y.; Liu, C.; Lu, X.H. Effects of filler crystal structure and shape on the tribological properties of PTFE composites. *Wear* **2007**, *40*, 1195–1203. [[CrossRef](#)]
19. Huang, T.; Li, T.; Xin, Y.; Liu, P.; Su, C. Mechanical and tribological properties of hybrid fabric-modified polyetherimide composites. *Wear* **2013**, *306*, 64–72. [[CrossRef](#)]
20. Zhang, H.; Li, M.; Zhou, Z.; Shen, L.; Bao, N. Microstructure and morphology control of potassium magnesium titanates and sodium iron titanates by molten salt synthesis. *Materials* **2019**, *12*, 1577. [[CrossRef](#)]
21. Zheng, H.; Shao, Y.; Wang, Y.; Meng, G.; Liu, B. Reinforcing the corrosion protection property of epoxy coating by using graphene oxide–poly(urea-formaldehyde) composites. *Corros. Sci.* **2017**, *123*, 267–277. [[CrossRef](#)]
22. Qiu, S.; Chen, C.; Cui, M.; Li, W.; Zhao, H.; Wang, L. Corrosion protection performance of waterborne epoxy coatings containing self-doped polyaniline nanofiber. *Appl. Surf. Sci.* **2017**, *407*, 213–222. [[CrossRef](#)]
23. GB/T 9286-1998. *Paints and Varnishes – Cross Cut Test for Films*; CHINESE GB Standards: Beijing, China, 1998.
24. GB/T 6739-2006. *Paints and Varnishes - Determination of Film Hardness by Pencil Test*; CHINESE GB Standards: Beijing, China, 2006.
25. GB/T 1732-1993. *Determination of Impact Resistance of Films*; CHINESE GB Standards: Beijing, China, 1993.
26. Hu, Y.; Li, C.; Shen, L.; Bao, N. Preparation of ferric sodium titanate whisker /FEVE composite coating and its wear and corrosion resistance. *Surf. Technol.* **2017**, *12*, 71–77.
27. Chang, L.; Zhang, Z.; Ye, L.; Friedrich, K. Tribological properties of high temperature resistance polymer composites with fine particles. *Tribol. Int.* **2007**, *40*, 1170–1178. [[CrossRef](#)]
28. Wang, Y.; Yan, F. Tribological properties of transfer film of PTFE-based composites. *Wear* **2006**, *261*, 1359–1366. [[CrossRef](#)]
29. Song, H.J.; Zhang, Z.Z.; Men, X.H.; Luo, Z.Z. A study of the tribological behavior of nano-ZnO<sub>2</sub>-filled polyurethane composite coatings. *Wear* **2010**, *269*, 79–85. [[CrossRef](#)]



© 2019 by the authors. Licensee MDPI, Basel, Switzerland. This article is an open access article distributed under the terms and conditions of the Creative Commons Attribution (CC BY) license (<http://creativecommons.org/licenses/by/4.0/>).